Supporting information

Tracking the Dynamic Histone Methylation of H3K27 in Live Cancer Cells

Ya Gong[1], Chujun Wei[1], Leonardo Cheng[1], Fengyi Ma[1], Shaoying Lu[1], Qin Peng[1], Longwei Liu[1*], Yingxiao Wang[1*]

1. Department of Bioengineering, Institute of Engineering in Medicine, University of California, San Diego, 9500 Gilman Drive, La Jolla, CA, 92093-0435, USA

* Corresponding authors: Yingxiao Wang, yiw015@eng.ucsd.edu; Longwei Liu, lol001@eng.ucsd.edu

Table of contents:

Supplementary Figures

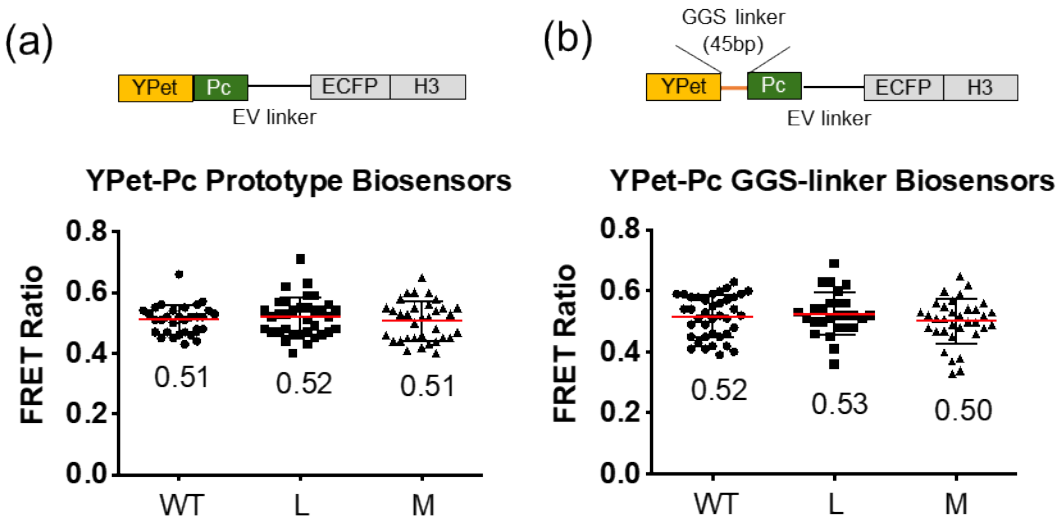

Supplementary Figure 1. Swapping the positions of YPet and Pc domains in the biosensors with (a) or without (b) GGS linkers both diminished the performance of the GGS-linker and prototype biosensors (One-way ANOVA test, all these groups have no significant difference). Red line indicates the mean value in all figures.

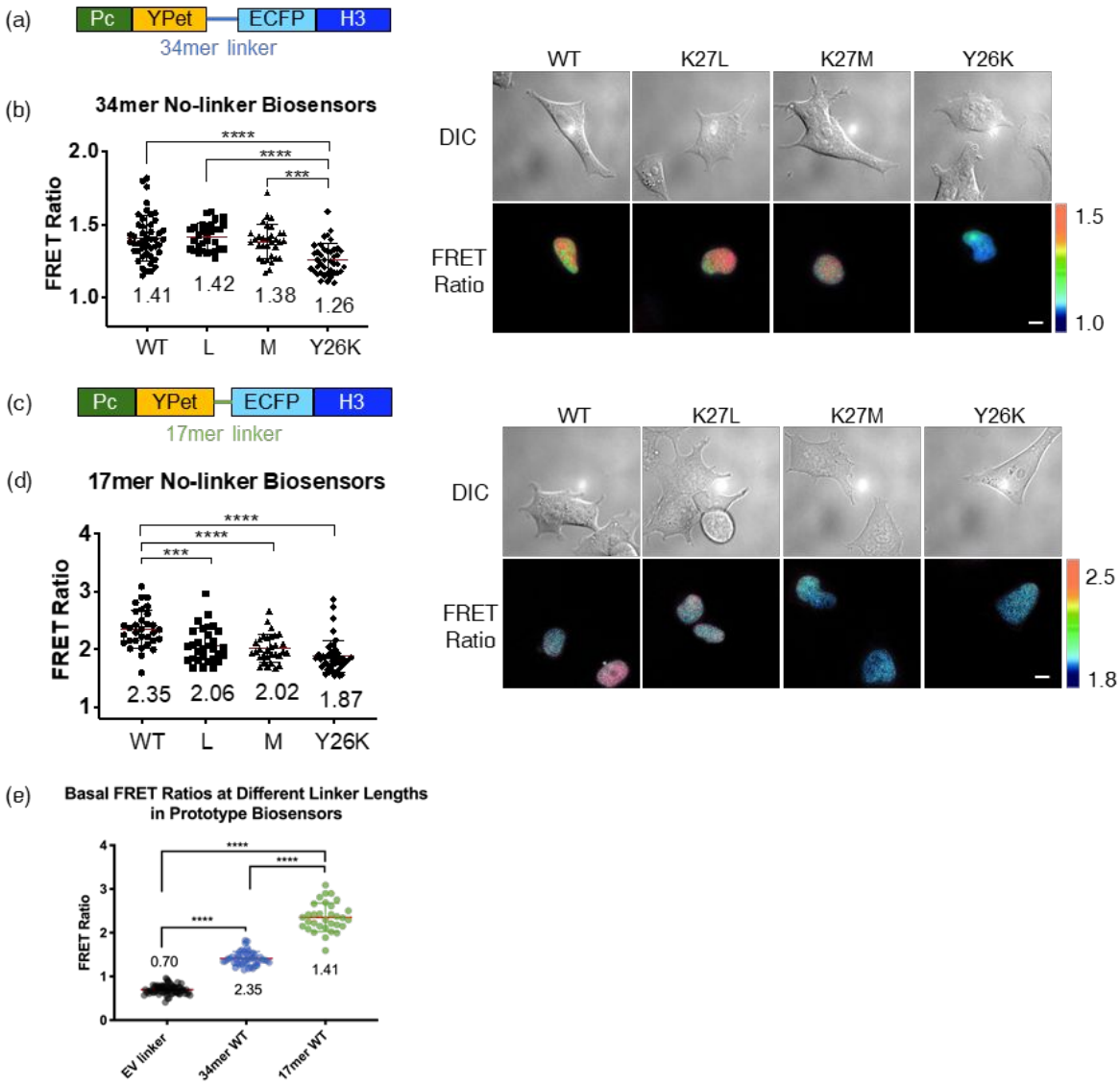

Supplementary Figure 2. Varying the length of the primary linker in the prototype biosensor without the 15mer GGS linker can affect the biosensor sensitivity.

(a) The schematic presentation of the 34mer prototype biosensor.
(b) The averaged FRET ratios of the wild-type and mutant 34mer prototype biosensors (K27L, K27M, Y26K) (upper panel) and their DIC (middle panel) and FRET ratio images (bottom panel) in HEK cells. (One-way ANOVA test, *** $p<0.001$, **** $p<0.0001$).
(c) A schematic drawing of the 17mer prototype biosensor.
(d) The averaged FRET ratios of the wild-type and mutant 17mer prototype biosensors (K27L, K27M, Y26K) (upper panel) and their DIC (middle panel) and FRET ratio images (lower panel) in HEK cells (One-way ANOVA test, *** $p<0.001$, **** $p<0.0001$).
(e) Comparison of the FRET ratios among the wild-type EV-linker, 34mer and 17mer prototype biosensors expressed in HEK cells. (One-way ANOVA test, **** $p<0.0001$). (Scale bar 10µm.)

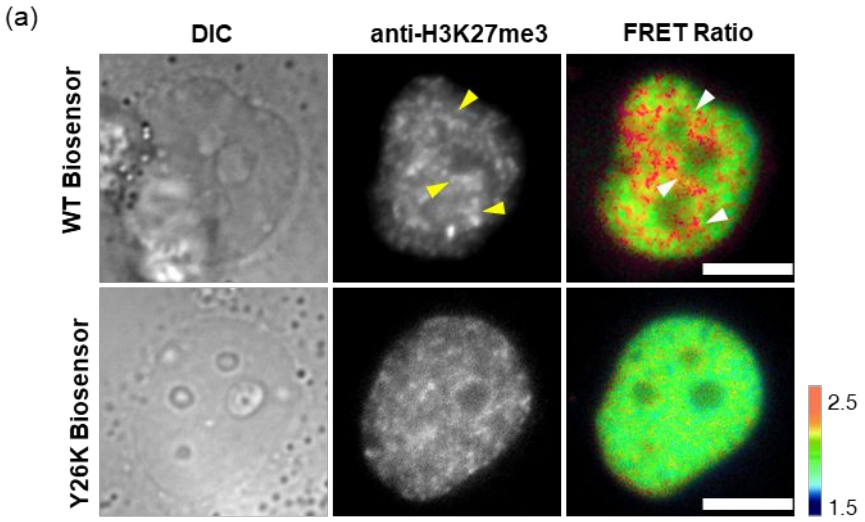

Supplementary Figure 3. The spatial distribution of H3K27me3 in nucleus.

(a). The representative images of H3K27me3 distribution in the nucleus as represented by the immunofluorescence staining assay (middle) and FRET imaging (right). In contrast to the control mutant biosensor, the wild-type biosensor showed a clear correlation with the immunofluorescence staining by an antibody in the nucleus (Scale bar = 10 μm) .

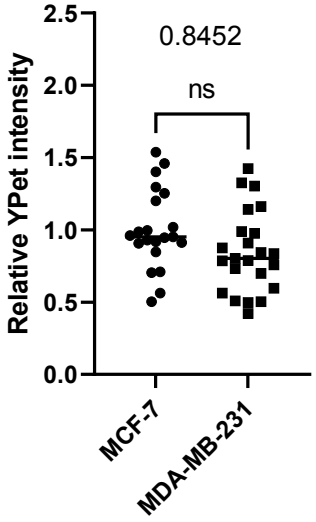

Supplementary Figure 4. Quantification of biosensor expression in different cell types.

The biosensor expression is represented by the relative YPet intensity in the nucleus. No significant difference was found between these two groups. (n=21 and 23, respectively, Student's t-test, ns p=0.8452).

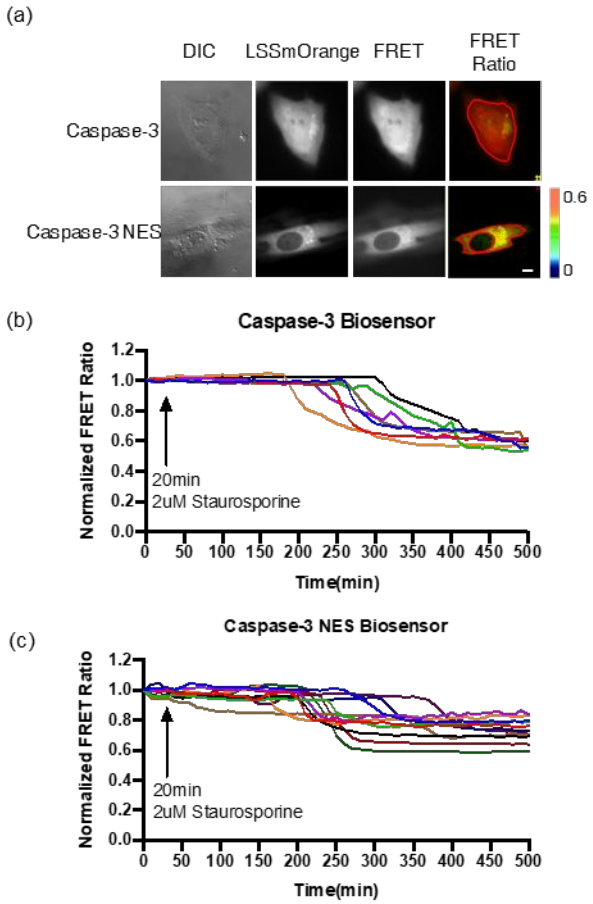

Supplementary Figure 5. Characterization of the Caspase-3 NES biosensor

(a) Images of the Hela cells with either caspase 3 biosensor (Upper) and caspase-3 NES biosensor (Lower) taken in DIC, LSSmOrange, FRET channels and their FRET ratio images.

(b-c) The FRET ratio changes of the caspase-3 biosensor (b) or the caspase-3 NES biosensor (c) in Hela cells after the induction of cell apoptosis by staurosporine. FRET ratio images were taken every 10 minutes.

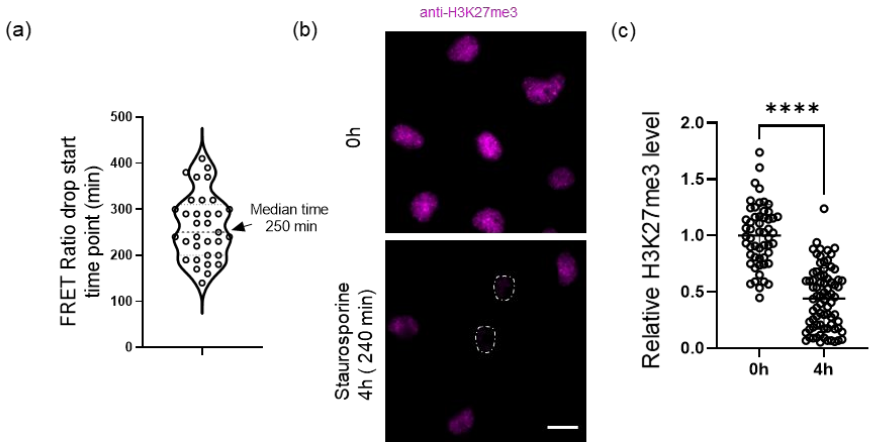

Supplementary Figure 6. Demethylation of H3K27 during apoptosis.

(a). Quantification of demethylation start time point measured by the FRET assay in live cell imaging. The median time of FRET ratio drop is 250 min.

(b-c). The representative images (b) and quantification (c) of H3K27me3 in immunofluorescence staining assay. Significant demethylation was found after staurosporine treatment for 4 hours (n=58 and 74, respectively in c, Student's t-test, $p<0.0001$). Scale bar = 20 μm in b.

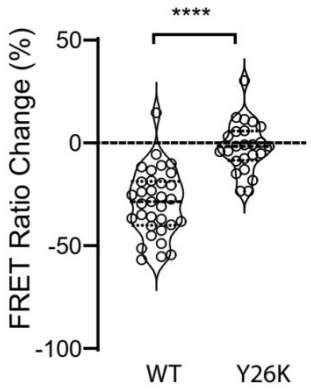

Supplementary Figure 7. The FRET ratio changes of the FRET biosensors in apoptotic cells.

The FRET Ratio change of wild type or Y26K mutant biosensors in the HeLa cells after staurosporine treatment for 4 hr. (n=33 and 24, respectively, Student's t-test, ****$p<0.0001$).